



Comparison of shell side mass transfer correlations in randomly packed hollow fiber membrane modules

Shufeng Shen, Kathryn H. Smith, Sandra E. Kentish, Geoff W. Stevens*

The Particulate Fluids Processing Centre, Department of Chemical and Biomolecular Engineering, The University of Melbourne, Parkville, Victoria 3010, Australia

Tel. +61383446621; Fax +61383448824; email: gstevens@unimelb.edu.au

Received 31 July 2009; accepted 15 December 2009

ABSTRACT

In this work, the process of membrane-based solvent extraction was examined with 10% (v/v) tributyl phosphate in kerosene/phenol/water as experimental system, involving solute mass transfer from the aqueous phase (flowing in the shell or tube side) to the organic phase. Shell side mass transfer performance was determined in two randomly packed membrane modules with different packing densities. Experimental data of shell side mass transfer coefficient were compared with model predictions from nine existing empirical correlations. Results showed that the correlations of Gawronski et al. and Viegas et al. were found to give the good predictions in these modules.

Keywords: Hollow fiber membrane; Shell side mass transfer; Model prediction; Membrane contactor

1. Introduction

Phenol and its derivatives are often pollutants in the wastewater discharged by manufacturing processes such as in the petrochemical and agrochemical industries and in coal gasification wastewaters [1]. Due to their potential harm to human health, treatment processes must be implemented before the waste streams can be safely discharged.

In the literature, many researchers have extensively studied phenol recovery with hollow fiber membrane contactors in shell and tube configuration [2–6]. A number of empirical correlations have been proposed in the past two decades, each with restrictions on their range of application [5–16]. In these empirical correlations, the shell side mass transfer coefficient, expressed by Sherwood number, is a function of the Reynolds and Schmidt numbers with a wide range of

exponents. They display quite large discrepancies, in both the magnitude of mass transfer coefficient as well as the general predictive trends. Some correlations also include the effect of geometry, such as module length and packing density. Often, inconsistent or conflicting results are obtained from the use of comparable empirical equations [4–6, 9].

Our aim in this paper is to compare the observations and predictions from these empirical correlations of shell side mass transfer, and to give a general view of these discrepancies in different randomly packed membrane modules using a liquid–liquid extraction system of 10% (v/v) tributyl phosphate in kerosene/phenol/water.

2. Theory

2.1. Experimental shell side mass transfer coefficient

For phenol extraction in a hydrophobic membrane contactor, the mass transfer from the aqueous to the

*Corresponding author

Table 1
Empirical correlations for shell side mass transfer

Authors	Correlations	Conditions	Cited	Ref.
Prasad and Sirkar	$Sh_s = 5.85(1 - \phi) \left(\frac{d_h}{l}\right) Re^{0.60} Sc^{0.33}$	$0 < Re < 500; 0.04 < \phi < 0.4$	210	[9]
Costello et al.	$Sh_s = (0.53 - 0.58\phi) Re^{0.53} Sc^{0.33}$	$21 < Re < 324; 0.32 < \phi < 0.76$	110	[10]
Wu et al.	$Sh_s = (0.3045\phi^2 - 0.3421\phi + 0.15) Re^{0.90} Sc^{0.33}$	$32 < Re < 1290; 0.08 < \phi < 0.70$	44	[11]
Gawronski et al.	$Sh_s = 0.09(1 - \phi) Re^{(0.8-0.16\phi)} Sc^{0.33}$	$0 < Re < 10; 0.21 < \phi < 0.80$	32	[12]
Lipnizki et al.	$Sh_s = 1.615 \left(1 + 0.14(\sqrt{\phi})^{-0.5}\right) \left(\frac{d_h}{l}\right)^{1/3} Re^{1/3} Sc^{1/3}$	Laminar flow	34	[13]
Asimakopoulou et al.	$Sh_s = 1.615(0.6 + 1.7\phi) \left(\frac{d_{out}}{l}\right)^{1/3} Re^{1/3} Sc^{1/3}$	$3 < Re < 78; 0.05 < \phi < 0.45$	3	[14]
Zheng et al.	$Sh_s = (0.163 + 0.27\phi) G_z^{0.60}$	$178 < Re < 1194; 0.20 < \phi < 0.50$	11	[15]
Viegas et al.	$Sh_s = 8.71 \left(\frac{d_h}{l}\right) Re^{0.74} Sc^{0.33}$	$0.16 < Re < 7.30; \phi = 0.3024$	45	[16]
Yang and Cussler	$Sh_s = 1.25 \left(Re \frac{d_h}{l}\right)^{0.93} Sc^{0.33}$	$0.5 < Re < 500; 0.02 < \phi < 0.33$	247	[17]

organic phase can be described with the conventional resistance-in-series model [5–8]. If equilibrium distribution at the interface was very fast, the following expressions apply:

Aqueous phase flows in tube side

$$\frac{1}{K_{aq}} = \frac{1}{k_t} + \frac{d_{in}}{Dk_m d_{lm}} + \frac{d_{in}}{Dk_s d_{out}} \quad (1)$$

Aqueous phase flows in shell side

$$\frac{1}{K_{aq}} = \frac{d_{out}}{Dk_t d_{in}} + \frac{d_{out}}{Dk_m d_{lm}} + \frac{1}{k_s} \quad (2)$$

where k_t , k_m and k_s are the local mass transfer coefficient in the aqueous tube side, through the membrane pores and on the organic shell side, respectively. D is the distribution ratio. d_{in} , d_{lm} and d_{out} are the inner, log mean and outside diameters of the hollow fiber, respectively.

In this work, two fluids in the membrane contactor were operated in a once-through mode. The overall mass transfer coefficient can be defined by considering an overall mass balance based on the aqueous phase side along the module [8]:

$$-Q_{aq} dc_{aq} = K_{aq} (c_{aq} - c_{aq}^*) dA \quad (3)$$

$$K_{aq} = \frac{Q_{aq}}{A_m} \ln \left(\frac{c_{aq}^{in}}{c_{aq}^{out}} \right) \quad (4)$$

where K_{aq} is the overall mass transfer coefficient. c_{aq}^* is the concentration of solute in the aqueous phase that

would be in equilibrium with the solute concentration in the organic phase at the same time and position. A_m is the effective interfacial area.

The values of shell side mass transfer coefficient could be deduced combining the calculated k_t and k_m with the experimental values of K_{aq} .

Aqueous phase flows in tube side

$$k_s = \frac{d_{in}}{Dd_{out}} \left(\frac{1}{K_{aq}} - \frac{1}{k_t} - \frac{d_{in}}{Dk_m d_{lm}} \right)^{-1} \quad (5)$$

Aqueous phase flows in shell side

$$\frac{1}{k_s} = \frac{1}{K_{aq}} - \frac{d_{out}}{Dk_t d_{in}} - \frac{d_{out}}{Dk_m d_{lm}} \quad (6)$$

Tube side:

$$Sh_t = \frac{k_t d_{in}}{D_d} = 1.62 Sc^{1/3} Re^{1/3} \left(\frac{d_{in}}{l} \right)^{1/3} \quad (G_z > 6), \quad (7)$$

where Sh , Re and Sc are the Sherwood, Reynolds and Schmidt numbers, respectively. D_d is the diffusivity of solute, and l is the length of fibers [7].

Membrane: The transmembrane mass transfer coefficient can be calculated from the membrane parameters of porosity (ϵ), tortuosity (τ) and thickness as well as solute diffusivity (D_{org}) as follows [7]:

$$k_m = \frac{2\epsilon D_{org}}{\tau(d_{out} - d_{in})} \quad (8)$$

Table 2
Module characteristics and parameters used in calculation

Module characteristics	No. 1	No. 2
Contactor inside diameter, m	0.0075	0.0075
Number of fibers, N	70	81
Effective length of fiber, L, m	0.21	0.20
Packing fraction, ϕ	0.37	0.43
Physical properties [5]		
Viscosity of aqueous phase, μ , cP (22°C)	0.98	
Viscosity of organic phase, μ , cP (22°C)	1.75	
Diffusivity of phenol, $m^2 s^{-1}$	1.051×10^{-9}	
Diffusivity of TBP-phenol, $m^2 s^{-1}$	3.492×10^{-10}	

2.2. Predictions of shell side mass transfer coefficient

The empirical correlations often cited in the literature are summarized in Table 1. In these correlations, the shell side mass transfer coefficient, expressed by the Sherwood number, could be predicted by using correlations of the general form [5]:

$$Sh_s = Af(\phi) \left(\frac{d_h}{l}\right)^\alpha Re^\beta Sc^\gamma, \quad (9)$$

where A , α , β and γ are constants obtained from the experimental data. $f(\phi)$ is a function of packing fraction. d_h and l are the hydraulic diameter of shell side and length of fibers, respectively. It is assumed that all the empirical correlations are not restricted to their experimental conditions and can be extrapolated to the conditions used in this study.

3. Experimental

Two membrane modules used in this study were carefully fabricated by potting a desired number of hydrophobic polypropylene hollow fibers (Memtec, Australia) into a cylindrical glass tube in a shell and tube configuration.

The fibers are 0.545 mm OD and 0.255 mm ID. The porosity and tortuosity are estimated to 0.65 and 2.5, respectively. The characteristics of the membrane, modules and tested solution are presented in Table 2.

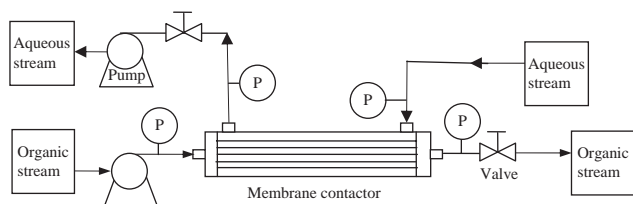


Fig. 1. Schematic diagram of experimental set-up.

A schematic diagram of experimental set-up in a counter-current once-through mode was shown in Fig. 1. In the module No. 1, the 10% (v/v) TBP in Shell-sol 2046 was pumped through the tube side and the aqueous phase flowed through the shell side. In the module No. 2, the aqueous phase flowed in the tube side. A slight overpressure (about 5 kPa) on the aqueous side was maintained to avoid organic breakthrough of the membrane. The experiments were performed by varying the flow rates of one phase and at specific flow rates of another phase. The phenol concentrations were analyzed by high performance liquid chromatography (Agilent 1200 HPLC). The mobile phase was a mixture of methanol and water (56%/44% (v/v)) at a flow rate of 1.0 ml min^{-1} .

4. Results and discussion

4.1. Comparison between the observed and predicted shell side mass transfer coefficient

Extraction equilibrium showed that the distribution ratios were constant ($D = 33.50 \pm 2.0$) in the system of 10% (v/v) TBP in Shellsol/phenol/ water at pH 5.0–7.0. This value is consistent with our previous results [5]. The experimental data of shell side mass transfer coefficient in membrane contactor No. 1 were compared with the predicted values calculated from empirical correlations, as shown in Fig. 2.

The flow rates in the shell side were varied within the range of $3.87\text{--}15.96 \text{ mL min}^{-1}$ while the flow rate of organic phase in the tube side was kept constant ($G_z = 25$). It can be found that the experimental shell side mass transfer coefficients increased slightly as the Re_{aq} increased from 2.2 to 8.9. The corresponding Sherwood numbers changed from 1.22 to 2.46. However, the predicted values vary in a very wide range from 1.0×10^{-7} to $9.0 \times 10^{-6} \text{ m s}^{-1}$. The predicted values from the correlations proposed by Costello et al. [10], Lipnizki et al. [13] and Asimakopoulou et al. [14] were much greater than the experimental data. However, the correlation by Prasad and Sirkar [9] and Yang and Cussler [17] underestimated greatly. In case of Gawronski et al. [12], Zheng et al. [15], Wu et al. [11] and Viegas et al. [16], the correlations predicted the values reasonably close to all experimental data in this work.

The observed K_{aq} and the predictions are plotted against the Reynolds number of aqueous phase (Re_{aq}) as shown in Fig. 3. Results from resistance-in-series model indicate that the shell side contributes major resistance (>80%) in this process. It can be seen that the experimental overall mass transfer coefficients ranged from 1.2×10^{-6} to $2.5 \times 10^{-6} \text{ m s}^{-1}$ and generated a similar trend with the predicted curves with the

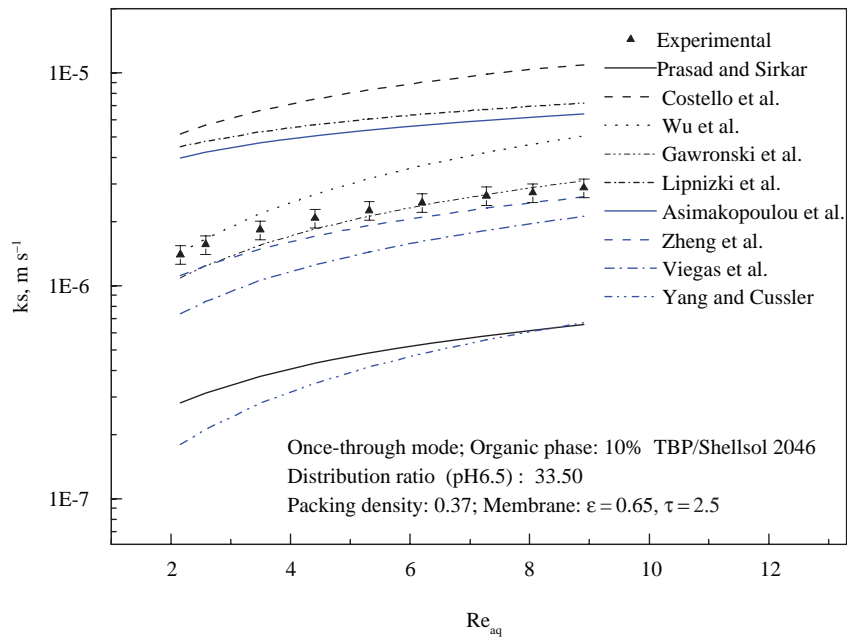


Fig. 2. Comparison between the experimental and predicted shell side mass transfer coefficient.

increasing Re_{aq} on the shell side. The predictions using the correlation of Gawronski et al. matched well with the experimental data.

4.2. Validation in different modules

A set of experiments were carried out in a different membrane module (No. 2) and different operation mode in order to validate performance of the better correlations observed in the module No. 1. The experimental and predicted results were shown in Fig. 4.

In this module, the organic phase flowed in the shell side. It can be seen from the Fig. 4 that there was a wide range of discrepancies between the experiment and the predictions. The predicted Sherwood number from the two correlations of Gawronski et al. and Viegas et al. agreed well with the experimental data. Model predictions from correlations of Costello et al., Lipnizki et al. and Asimakopoulou et al. had large positive discrepancies. The correlation of Prasad and Sirkar and Dahuron and Cussler also gave poor predictions. These observations were consistent with the aforementioned results in the module No. 1.

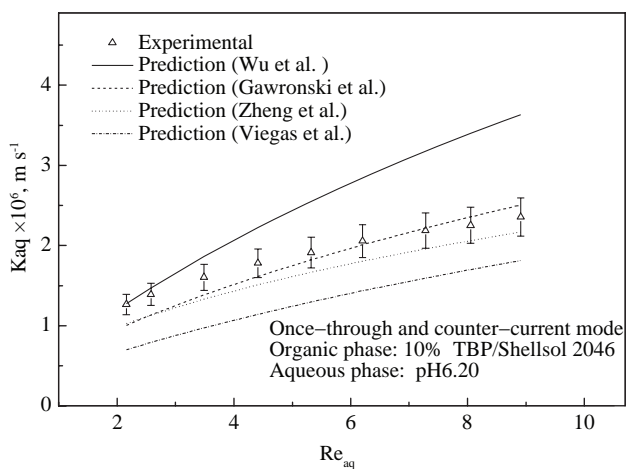


Fig. 3. Discrepancies between the observed overall mass transfer coefficient and model prediction.

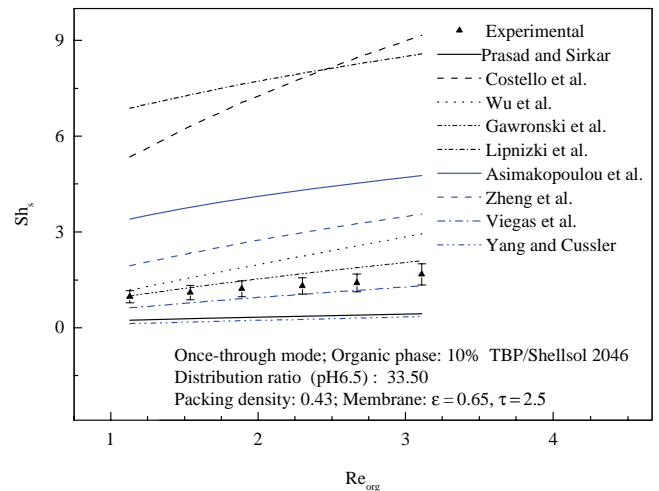


Fig. 4. Comparison between the experimental Sherwood numbers and the predicted values in the module No.2.

The results reported above indicate that the correlation of Gawronski et al. predicted well the performance of the two modules and the correlation of Viegas et al. underestimated the mass transfer rate but within 30%. It is noted that the experimental conditions are similar to the boundary of these two correlations. Moreover, the correlations of Gawronski et al. and Viegas et al. were also proposed from the results in liquid–liquid extraction systems. The other correlations except for the correlation of Prasad and Sirkar were correlated in gas–liquid experimental systems where liquid phase flowed through the shell side and the shell side mass transfer coefficients were considered to be controlling.

Therefore, in the case of a liquid–liquid system in a membrane module with ϕ around 0.40, shell side mass transfer can be estimated from the empirical correlations of Gawronski et al. and Viegas et al.

5. Conclusions

In this work, the empirical correlations for shell side mass transfer in membrane contactors were summarized. Experimental data were compared to existing model predictions in two different modules. Consistent results were observed. The correlations of Gawronski et al. and Viegas et al. were recommended to predict shell side mass transfer in a randomly packed hollow fiber module.

Acknowledgement

The authors would like to thank the Australian Research Council (ARC), GlaxoSmithKline Australia Ltd. (GSK) and the Particulate Fluids Processing Centre, a Special Research Centre of the Australian Research Council, for financial support.

Symbols

A	Membrane area of mass transfer, m^2
C	Phenol concentration, g /L
D	Distribution ratio
d_{in}	Inner diameter of hollow fiber membrane, m
d_h	The hydraulic diameter of shell side, m
d_{lm}	Logarithmic mean diameter of hollow fiber, m
d_{out}	Outer diameter of hollow fiber membrane, m
D_{aq}	Diffusivity of phenol in aqueous phase, m^2/s
D_d	Diffusivity of solute, m^2/s
D_{org}	Diffusivity of the organic phase, m^2/s
K	Local mass transfer coefficient, m/s

K	Overall mass transfer coefficient, m/s
l	Length of hollow fiber, m
Q_{aq}	Flow rate of the aqueous phase, m^3/s
Re	Reynolds number
Sc	Schmidt number
Sh	Sherwood number

Greek

ε	membrane porosity
μ	viscosity (kg/m s)
ρ	density (kg/m ³)
τ	tortuosity of membrane pores
ϕ	The packing fraction of membrane contactor

Subscripts

aq	aqueous
m	membrane
org	organic
s	shell
t	tube

Superscripts

*	Equilibrium concentration between two phases.
---	---

References

- [1] C. Yang, Y. Qian, L. Zhang and J. Feng, Chem. Eng. J., 117 (2006) 179–185.
- [2] M.J. González-Muñoz, S. Luque, J.R. Álvarez and J. Coca, J. Membr. Sci., 213 (2003) 181–193.
- [3] W. Cichy, S. Schlosser and J. Szymanowski, Solv. Ext. Ion Exch., 19(5) (2001) 905–923.
- [4] M.C. Figueroa and M.E. Weber, Sep. Sci. Technol. 40 (2005) 1653–1672.
- [5] S.F. Shen, K.H. Smith, S. Cook, S.E. Kentish, J.M. Perera, T. Bowser and G.W. Stevens, Sep. Purif. Technol., 69 (2009) 48–56.
- [6] R. Basu, R. Prasad and K. K. Sirkar, AIChE J., 36 (1990) 450–460.
- [7] A. Gableman and S.T. Hwang, J. Membr. Sci., 159 (1999) 61–106.
- [8] E.A. Fouad and H.J. Bart, Solv. Extra. Ion Exch., 25(2007) 857–877.
- [9] R. Prasad and K.K. Sirkar, AIChE J., 34(2) (1988) 177–188.
- [10] M.J. Costello, A.G. Fane, P.A. Hogan and R.W. Schofield, J. Membr. Sci., 80 (1993), 1–11.
- [11] J. Wu and V. Chen, J. Membr. Sci., 172 (2000) 59–74.
- [12] R. Gawronski and B. Wrzesinska, J. Membr. Sci., 168 (2000) 213–222.
- [13] F. Lipnizki and R.W. Field, J. Membr. Sci., 193 (2001) 195–208.
- [14] A.G. Asimakopoulou and A.J. Karabelas, J. Membr. Sci., 271 (2006) 151–162.
- [15] J.M. Zheng, Y.Y. Xu and Z.K. Xu, Sep. Sci. Technol., 38 (2003) 1247–1267.
- [16] R.M.C. Viegas, M. Rodríguez, S. Luque, J.R. Alvarez, I.M. Coelho and J.P.S.G. Crespo, J. Membr. Sci., 145 (1998) 129.
- [17] M. Yang and E.L. Cussler, AIChE J., 32(11) (1986) 1910–1916.